Published in final edited form as:
Nucl Med Biol. 2012 October ; 39(7): 905–915. doi:10.1016/j.nucmedbio.2012.05.003.

Characterization of ^{99m}Tc-labeled cytokine ligands for inflammation imaging via TNF and IL-1 pathways

Zhonglin Liu[a,*], **Leonie wyffels**[a,†], **Christy Barber**[a], **Li Wan**[a], **Hua Xu**[b], **Mizhou M. Hui**[c], **Lars R. Furenlid**[a], and **James M. Woolfenden**[a]

[a]Department of Medical Imaging, University of Arizona, Tucson, AZ

[b]Department of Pediatrics, University of Arizona, Tucson, AZ

[c]AmProtein Inc., San Gabriel, CA

Abstract

Introduction—TNFR2-Fc and IL-1ra-Fc are recombinant cytokine ligands that target TNF and IL-1. TNFR2-Fc-IL-1ra, a dual-domain agent that incorporates both ligands, allows bifunctional binding of IL-1 receptors and TNF. This study was designed to characterize ^{99m}Tc-labeled forms of these ligands, ^{99m}Tc-IL-1ra-Fc (IF), ^{99m}Tc-TNFR2-Fc (TF), and ^{99m}Tc-TNFR2-Fc-IL-1ra (TFI), for inflammation imaging.

Methods—The cytokine ligands were labeled with ^{99m}Tc by a direct approach via 2-iminothiolane (2-IT) reduction at various 2-IT/protein molar ratios. *In vivo* inflammation targeting studies were carried out in a mouse ear edema model created by topical application of 12-O-tetradecanoyl-phorbol-13-acetate (TPA) on the right ear of ICR mice.

Results—Radiolabeling yields increased with increasing amounts of 2-IT. When the 2-IT/protein ratio reached 1000, the radiolabeling yield was greater than 90% without significant colloid production. TPA-treated ears showed high radioligand uptake, which was clearly detected by SPECT and autoradiographic imaging. The activities (%ID/g) in the inflamed and control ears at 3 hr after injection were 2.76±0.20 vs. 0.69±0.12 for IF, 5.86±0.40 vs. 2.86±0.61 for TF, and 7.61±0.86 vs. 1.99±0.31 for TFI (P<0.05 vs. controls). TFI showed significantly higher uptake in the inflamed ears compared to TF and IF (P<0.05). Blocking study results indicated specificity of radioligand binding with decreased radioactive uptake in the inflamed ears. Western blotting and ELISA analysis showed further confirmed a high expression of IL-1β and TNF-α in the inflamed ears.

Conclusions—^{99m}Tc-labeled cytokine ligands are a promising approach for detecting and understanding the inflammatory process. TFI may be more useful than the single-domain ligands for noninvasive detection of inflammatory sites.

Keywords

^{99m}Tc; Cytokines; Interleukin-1; Tumor necrosis factor; Inflammation; Imaging

[*]Corresponding author: P.O. Box 245067, Tucson, AZ 85724-5067, Tel: (520) 626-4248; Fax: (520) 626-2892, zliu@radiology.arizona.edu.
[†]Present address: Department of Nuclear Medicine, University Hospital Antwerp, Edegem, Belgium

1. Introduction

Pro-inflammatory cytokines are associated with many systemic diseases, such as arthritis, atherosclerosis, and myocardial ischemia-reperfusion injury. Interleukin-1 (IL-1) is one of the most pleiotropic cytokines and causes a wide variety of biological effects related to inflammation, infection and autoimmune processes [1, 2]. IL-1 consists of two distinct proteins called IL-1α and IL-1β. As an agonist of IL-1 receptor (IL-1r), the action of IL-1 is regulated by the structurally-related IL-1r antagonist (IL-1ra), which is primarily produced by activated monocytes and tissue macrophages, as well as a variety of other cell types [3, 4]. IL-1ra is a specific receptor antagonist that competes for receptor binding with IL-1α and IL-1β, blocking their role in immune activation; it binds to cell membrane type I IL-1 receptor (IL-1RI) and prevents IL-1 from binding to the same IL-1 receptor [4, 5]. IL-1ra has no agonist activity and does not initiate signal transduction. A recombinant, nonglycosylated form of human IL-1ra, anakinra (Kineret®), has been approved by the U.S. Food and Drug Administration (FDA) for treatment of rheumatoid arthritis (RA) [6]. IL-1ra has been shown promise as a probe for experimental investigation of inflammation and as a potential novel therapeutic in IL-1 mediated inflammatory diseases, including cancer [6, 7].

Tumor necrosis factor (TNF) is another pro-inflammatory cytokine that possesses significant inflammatory activity. There are 2 types of TNF, TNF-α and TNF-β, which are mammalian-secreted proteins capable of inducing a wide variety of effects on a large number of cell types. TNF-α is essential in initiating inflammatory reactions in the body and is involved in triggering and/or amplifying local inflammatory responses [8].

TNF initiates its biological effects by binding to TNF receptors (TNFRs) expressed on the plasma membrane of a TNF-responsive cell. There are two distinct forms of TNFR: Type I TNFR (TNFR1) and Type II TNFR (TNFR2). The TNF receptors undergo proteolytic cleavage and release a fragment called soluble TNF receptor (soluble TNFR1 or TNFR2), which is a natural antagonist of TNF [9]. Soluble forms of cytokine receptors normally participate in control of cytokine activity *in vivo* by reducing the availability of cytokines to bind to their receptors [10, 11].

Experimental findings have demonstrated the important roles of TNF-α and IL-1β in the inflammatory process associated with many diseases. These two key pro-inflammatory cytokines may have coordinated effects [12–16]. For example, TNF-α, which alone has no effect on nitric oxide (NO) production in myocytes, greatly potentiates IL-1β-induced NO production [17]. Experimental therapy with inhibitors of both TNF-α and IL-1 showed more effective than therapy with either type of inhibitor alone in animal models of arthritis. It was found that combined anti-TNF-α and IL-1 treatment provided synergistic benefits and improved the outcome of arthritis in such a way that neutralization of both cytokines lead to both diminished inflammation and diminished cartilage damage [18–20]. The synergistic effects of the two cytokines suggest that strategies targeting multiple pro-inflammatory pathways simultaneously may be more effective than those that target a single pathway.

Radiolabelled cytokines, cytokine ligands, and monoclonal antibodies are an emerging class of radiopharmaceuticals for inflammation imaging [21]. This study was designed to validate three technetium-99m (^{99m}Tc) labeled cytokine ligands, ^{99m}Tc-TNFR2-Fc, ^{99m}Tc-IL-1ra-Fc, and ^{99m}Tc-TNFR2-Fc-IL-1ra, for inflammation imaging. TNFR2-Fc is a dimeric fusion protein composed of the ligand-binding portion of the human TNF receptor 2 (TNFR2) linked to the Fc portion of human IgG1 [22]. Fc-fusion soluble cytokine receptors are known to have improved retention of their biological activities and have shown more significant therapeutic value [23]. Under the name etanercept (Enbrel®), TNFR2-Fc has been approved by FDA for treatment of rheumatoid arthritis, psoriasis, ankylosing spondylitis, and psoriatic

arthritis [24]. The usefulness of ^{18}F-radiolabeled TNFR2-Fc for PET imaging of TNF-α expression has been previously reported in animal studies [25]. We radiolabeled TNFR2-Fc with ^{99m}Tc and investigated the feasibility of ^{99m}Tc-TNFR2-Fc for SPECT imaging using a mouse ear edema model. In principle, targeting endogenous IL-1 receptors with radiolabeled IL-1ra may provide a suitable approach for specific detection of inflammatory sites mediated by IL-1 receptor. Nevertheless, natural IL-1ra often exhibits short biological half-life and is rapidly cleared by the liver and kidneys. An ideal radioligand for SPECT imaging of IL-1 receptor expression should bind specifically to the receptors with high affinity and long-enough residence at the sites of inflammation to allow for optimal imaging. In this study, IL-1ra-Fc, a fusion protein containing IL-1ra and the Fc fragment, was radiolabeled with ^{99m}Tc to detect inflammatory response via IL-1 pathway.

Development of bispecific cytokine radioligands presents an attractive strategy to combine the effects of two cytokine pathways. The potential for using the synergistic effects of cytokines has motivated us to develop a radiolabeled dual-domain cytokine ligand, ^{99m}Tc-TNFR2-Fc-IL-1ra, for noninvasive assessment of inflammation and response to therapy in inflammatory and autoimmune diseases [26]. The recombinant human dual-domain TNFR2-Fc-IL-1ra contains an amino-terminal segment that specifically binds to TNF, as well as a carboxy-terminal segment with the sequence of IL-1ra that specifically binds to cell-membrane-bound IL-1 receptors. The Fc portion of human IgG1 links the two segments and is capable of dimerizing. A schematic view of TNF and IL-1 receptor expression, ligands, interactions, and ^{99m}Tc-TNFR2-Fc-IL-1ra binding mechanism is shown in Figure 1. We expected that ^{99m}Tc-TNFR2-Fc-IL-1ra could target inflammatory sites with more potent affinity and increased radioactive uptake in comparison with individual cytokine radioligands, ^{99m}Tc-TNFR2-Fc and ^{99m}Tc-IL-1ra-Fc.

2. Materials and Methods

2.1. Production of IL-1ra-Fc and TNFR2-Fc-IL-1ra

IL-1ra-Fc and TNFR2-Fc-IL-1ra, which are fusion proteins derived from recombinant DNA, were developed at AmProtein Corporation (Camarillo, CA). Two genes that originally coded for human IL-1ra and IgG1 Fc fragment were fused to produce a hybrid gene for IL-1ra-Fc. Similarly, three genes for TNFR2, Fc fragment, and IL-1ra were linked together to produce another hybrid gene for TNFR2-Fc-IL-1ra Translation of each fusion gene resulted in a single polypeptide with functional properties derived from the original individual proteins. Production of IL-1ra-Fc and TNFR2-Fc-IL-1ra was accomplished by the large-scale culturing of Chinese hamster ovary (CHO) cells that have been cloned to express the recombinant DNA construct. The cells were cultured in a serum-free suspension system with CHO-CD4 medium (Irvine Scientific, Santa Ana, CA) and in-house feed medium, and scaled up in a 3-liter bioreactor (Applikon Biotechnology, Foster City, CA). The protein was purified by Protein-A direct capture, followed by ion-exchange and hydrophobic chromatography. The purified protein was further processed and analyzed by size-exclusion and high-performance liquid chromatography (SEC-HPLC).

2.2. Radiolabeling

TNFR2-Fc (anakinra, Kineret®) was purchased from Amgen Inc. (Thousand Oaks, CA). Glucoheptonic acid (GH) and 2-iminothiolane (2-IT) were purchased from Sigma Aldrich, Inc. (St Louis, MO). IL-1ra-Fc, TNFR2-Fc, and TNFR2-Fc-IL-1ra were radiolabeled with ^{99m}Tc using a modified direct labeling protocol as previously described [27–29] in which GH serves as a transfer agent to chelate tin-reduced $^{99m}TcO_4^-$ to thiolated proteins. Optimal ratios of 2-IT to protein were determined in a series of direct ^{99m}Tc-labeling experiments with IL-1ra-Fc, TNFR2-Fc, and TNFR2-Fc-IL-1ra. A total of 100 μg protein in

100 μL PBS was incubated with 20 μL 2-IT in saline at 2-IT/protein ratios of 20, 200, 1000, and 2000, respectively, for 30 minutes at 37°C. A freshly prepared 5μL $SnCl_2$ solution (1 mg/mL in nitrogen-purged 0.1 N HCl) was mixed with 200 μL GH solution (0.5 mg/mL in nitrogen-purged saline). Three hundred μL of $^{99m}TcO_4^-$ (25–30 mCi) in 0.9% NaCl was added to the stannous glucoheptonate mixture and incubated at room temperature for 5 minutes to produce ^{99m}Tc-glucoheptonate. The thiolated protein was added into the vial of ^{99m}Tc-glucoheptonate and incubated at room temperature for 30 minutes.

Radiolabeling efficiency (radiochemical purity, RCP) was determined by size-exclusion high performance liquid chromatography (SEC-HPLC) and ascending paper chromatography on Whatman silica gel-loaded chromatography paper (SG-81) (Whatman Int. Ltd., Maidstone, UK). SEC-HPLC was carried out using a Shodex KW 802.5 column (7.8 × 300 mm, 5 μm particle size) (Thomson Instrument Co., Oceanside, CA) and a Waters Breeze system (Waters Technologies Corp., Milford, MA) equipped with a Waters 1525 Binary HPLC Pump and a Waters 2489 dual absorbance detector (280 nm) in line with a Flow-Count™ Radio HPLC Flow Through Detector (Bioscan Inc., Washington, DC). The radiolabeled protein was eluted with 0.1 mol/L KH_2PO_4 at pH 7.0 at a flow rate of 0.8 mL/min.

The mobile phases for paper chromatography were 0.9% saline. In this saline solvent system, free $^{99m}TcO_4^-$ moves with the solvent front, leaving labeled and reduced/hydrolyzed (R/H) ^{99m}Tc at the point of application. R/H ^{99m}Tc was separated by using 5% bovine serum albumin (BSA)-impregnated Whatman SG81 paper strips as the stationary phase and solvent mixture ethanol:ammonia:water = 2:1:5 (v/v) as the mobile phase. In this system, free ^{99m}Tc and labeled proteins move with the solvent front, whereas R/H ^{99m}Tc remains at the point of application. Radiochromatograms of the paper strips were obtained using digital autoradiograph imaging. The strips were exposed to Fujifilm phosphor imaging plates for 1–5 minutes. A Fujifilm BAS-5000 Bio-Imaging Analysis System (Fujifilm Medical Systems USA, Stamford, CT) was used to scan the plates for digital autoradiograph collection. The strips were cut into 1-cm pieces and counted by a CRC-15W Dose Calibrator/Well Counter (Capintec, Ramsey, NJ).

For *in vitro* stability and *in vivo* animal studies, the radiolabeled products were purified using a disposable PD-10 desalting column pre-packed with Sephadex G-25 Medium (GE Healthcare, Piscataway, NJ). The column was pre-equilibrated and eluted with PBS, pH 7.4. Protein concentrations of collected fractions were determined using a Genesys 10 Bio spectrophotometer and BCA™ Protein Assay Kit (Thermo Fisher Scientific Inc., Rockford, IL).

2.3. *In vitro* and *in vivo* stability

Stability was representatively investigated in ^{99m}Tc-TNFR2-Fc-IL-1ra. *In vitro* stability study was first carried out by incubation of purified radiotracer in saline at room temperature and in rat serum at 37°C for 21 hours. Aliquots were taken and analyzed by SEC-HPLC and ascending paper chromatography at various time points (0h, 2h, 4h and 21h). In addition, cysteine challenge was performed by incubating purified ^{99m}Tc-TNFR2-Fc-IL-1ra with cysteine hydrochloride in phosphate buffer for 1 hour at 37°C as previously described in literature [30]. The molar ratios of cysteine to protein were 500, 100, 5, and zero. A fresh cysteine solution (10 mg/mL in 0.1M PBS, pH 7.0) was prepared each time and diluted to different concentrations. Each cysteine solution at 10 μL, or the same volume of PBS for the cysteine-free controls, was added to 100 μl of the labeled protein solution. At the end of 1-hour incubation, the RCP in each mixture was assessed by SEC-HPLC or paper chromatography as described above.

In vivo stability of ^{99m}Tc-TNFR2-Fc-IL-1ra was performed in two Sprague-Dawley rats that received intravenous injections of purified ^{99m}Tc-TNFR2-Fc-IL-1ra (4.0 mCi, 0.3 mL). Blood samples (0.5 mL) were collected at 60 and 180 minutes post-injection. The samples were first centrifuged at 5000 rpm for 5 min to separate plasma and cellular fractions. The cellular fractions were washed with 0.5 mL PBS and centrifuged again. Individual fractions were measured with the CRC-15W Dose Calibrator/Well Counter. The plasma was analyzed by SEC-HPLC.

2.4. Biodistribution measurements

Biodistribution studies of ^{99m}Tc-IL-1ra-Fc, ^{99m}Tc-TNFR2-Fc, and ^{99m}Tc-TNFR2-Fc-IL-1ra were performed in healthy male Sprague-Dawley rats (250–300 g, n=5 for each radiotracer) purchased from Charles River Laboratories (Wilmington, MA).

Three hours after intravenous injection of the radioligands (3.5–5.5 mCi, 0.25–0.35 mL), the animals were euthanized with an overdose of sodium pentobarbital. Blood, skeletal muscle, heart, lung, stomach, intestine, liver, spleen, and kidneys were harvested, weighed, and measured using the CRC-15W Dose Calibrator/Well Counter.

2.5. Blood clearance

^{99m}Tc-labeled TNFR2-Fc, IL-1ra-Fc, and TNFR2-Fc-IL-1ra (3.5–5.5 mCi, 0.2–0.3 mL) were intravenously injected in three groups of male Sprague-Dawley rats (250–300 g), respectively. Serial blood samples (200 μL) were collected from a carotid artery catheter at 0, 1, 3, 6, 10, 30, 60, 120, and 180 minutes after injection. Each volume of sample withdrawn was replaced with an equal volume of warm physiological saline solution. The samples were weighed and measured with the CRC-15W Dose Calibrator/Well Counter to determine percent injected dose per gram (%ID/g) at each time point. Blood-clearance curves were modeled using a nonlinear Curve-Fit Kinetic Equation by TableCurve 2D® software (Systat Software Inc., Chicago, IL).

2.6. Accumulation of ^{99m}Tc-labeled cytokine ligands in TPA-induced inflammation in mouse ear

ICR mice (10–15 weeks old) were purchased from Charles River Laboratories (Wilmington, MA). Targeting of ^{99m}Tc-labeled cytokine ligands was assessed using an ear edema model, which was produced in the mice by topical application of 2.0 μg 12-O-tetradecanoylphorbol-13-acetate (TPA) (Sigma Aldrich, Inc., St Louis, MO) dissolved in 20 μL of acetone and administered through a micropipette (10 μL) to both the inner and outer surface of the right ear [25, 31, 32]. The left ear was topically treated with 20 μL of acetone (vehicle) as a negative control. The thickness of each ear was repeatedly measured using a digital caliper before and after TPA treatment. Twenty-four hours after TPA treatment, ^{99m}Tc-labeled TNFR2-Fc or IL-1ra-Fc/TNFR2-Fc-IL-1ra (3.5–4.5 mCi, 0.3 mL) was injected intravenously. To determine the specificity of uptake of each radioligand in the inflamed area, blocking tests were carried out in an extra group of ICR mice with TPA-induced ear edema by intravenous injection of the appropriate non-radiolabeled cytokine ligand (500 μg, 0.2 mL) 30 minutes before matched radioligand administration.

The animals were imaged for 10 minutes using a small-animal SPECT imager, FastSPECT II, at 3 hours after radiotracer injection. The ears were localized in the center of the field of view. The animals were sacrificed after imaging, and TPA-treated (right) and controlled (left) ears were harvested and measured using the CRC-15W Dose Calibrator/Well Counter to determine the uptake of each radioligand in the ears. Representative ears were exposed to the Fujifilm phosphor imaging plates. Digital autoradiograph images were read out using the BAS-5000 system.

1.7. Western blot analysis of IL-1β, IL-1RI, and TNF-α

Mouse ears treated with TPA or vehicle were harvested, snap-frozen in liquid nitrogen and stored in a −80°C freezer. The frozen ears were cut into small pieces and homogenized in 1 mL of Whole Cell Lysate Buffer using a tissue homogenizer. The tissue homogenates were centrifuged at 10,000g at 4°C for 10 min. The supernatants were collected and centrifuged again at 10,000g at 4°C for 10 min. Protein concentration in the supernatant was determined using a Pierce BCA Protein Assay kit (Thermo Scientific, Rockford, IL). Tissue lysate (40 μg protein) was separated on PAGE gel, and then transferred to a nitrocellulose membrane. Rabbit polyclonal IL-1β antibody and IL-1RI antibody were purchased from Santa Cruz Biotechnology, Inc. (Santa Cruz, CA) for detection of IL-1β and IL-1RI. Rabbit polyclonal TNF-α antibody was obtained from Abcam PLC (San Francisco, CA) for detection of TNF-α. Goat anti-rabbit IgG-HRP antibody as secondary antibody was purchased from Santa Cruz Biotechnology, Inc.

2.8. ELISA detection of IL-1β and TNF-α

Snap-frozen ear tissues were homogenized in a cell extraction buffer (Invitrogen Corporation, Camarillo, CA) containing 10 mM Tris, pH 7.4, 100 mM NaCl, 1 mM EDTA, 1 mM EGTA, 1 mM NaF, 20 mM $Na_4P_2O_7$, 2 mM Na_3VO_4, 1% Triton X-100, 10% glycerol, 0.1% SDS, 0.5% deoxycholate, and 0.5% deoxycholate. Immediately before the tissue was processed, 1 mM phenylmethylsulfonyl fluoride (PMSF) and protease inhibitor cocktail (Sigma-Aldrich Corp., St. Louis, MO) were added into the cell extraction buffer. The tissue mixture was placed on ice, sonicated for 30 seconds, and incubated at 4°C for 10 minutes. The final homogenate was centrifuged at 20,000g at 4°C for 15 minutes. Protein concentration was determined using a BCA Protein Assay Kit (Thermo Scientific, Rockford, IL). The supernatant fraction was aliquoted and frozen at −80°C until solid-phase sandwich enzyme-linked immunosorbent assays (ELISA) were performed for determination of cytokine protein levels.

The levels of mouse IL-1β and TNF-α were determined using ELISA kits purchased from Invitrogen Corporation (Camarillo, CA). The IL-1β and TNFα ELISA assays were performed according to the manufacturer's protocols. Briefly, diluted samples and standards at 100 μL (IL-1) were transferred to the antibody-coated wells in a 96-well polyvinyl plate. The plates were incubated for 90 minutes at room temperature and the wells were washed with wash solution. A solution of enzyme-conjugated detection antibody was added. After a second incubation for 30 minutes and washing, a substrate solution containing tetramethylbenzidine/H_2O_2 was added. After 30-minute incubation, the stop solution (0.5 mol/L H_2SO_4) was added and the plates were read using a DTX 880 Multimode Detector (Beckman Coulter, Inc., Fullerton, CA) at a wavelength of 450 nm. The results of IL-1β and TNFα measurements were expressed as pg/ml and corrected for total protein (pg/mg).

2.9. Data analysis

All quantitative results were expressed as mean ± S.E.M. Comparisons between two variables were performed with one-way analysis of variance. Probability values less than 0.05 were considered significant.

2.10. Ethics

The animal experiments were performed in accordance with Principles of Laboratory Animal Care from the National Institutes of Health (NIH Publication 85–23, revised 1985) and were approved by the Institutional Animal Care and Use Committee (IACUC) at the University of Arizona.

3. Results

3.1. ^{99m}Tc-labeling of cytokine ligands

All three cytokine ligands were radiolabeled with ^{99m}Tc by increasing 2-IT/protein ratios. The reaction mixtures were analyzed with SEC-HPLC and SG81 paper chromatographic analysis before purification to evaluate radiolabeling efficiencies and to determine optimal labeling conditions. The radiolabeling yields increased with increasing amounts of 2-IT. Table 1 shows the results of radiolabeling yields of ^{99m}Tc-TNFR2-Fc, ^{99m}Tc-IL-1ra-Fc, and ^{99m}Tc-TNFR2-Fc-IL-1ra with varied 2-IT/protein ratios, based on paper chromatographic analyses using saline and ethanol:ammonia:water solvents. Paper chromatography showed that ^{99m}Tc-labeled protein and reduced ^{99m}Tc remained at the point of spotting, while free $^{99m}TcO_4^-$ moved towards the solvent front. In Ethanol/Ammonia/Water (2/1/5) solution as another mobile phase, labeled protein and $^{99m}TcO_4^-$ moved to front, but reduced/hydrolyzed (R/H) ^{99m}Tc remained at the loading point. Because the radiolabeling original yield was greater than 90% without significant colloid production at a 2-IT/protein ratio of 1000, we selected this 2-IT/protein ratio to radiolabel the three recombinant proteins for stability tests and animal studies. After gel purification using the PD-10 column, there was no significant movement of free ^{99m}Tc with the solvent front in the radiolabeled products. As a result, the RCP was always greater than 97% in gel-purified products. The specific activity was 297–409 MBq/nM for ^{99m}Tc-IL-1ra-Fc, 766–1034 MBq/nM for ^{99m}Tc-TNFR2-Fc, and 979–1161 MBq/nM for ^{99m}Tc-TNFR2-Fc-IL-1ra.

Representative SEC-HPLC chromatograms of ^{99m}Tc-TNFR2-Fc, ^{99m}Tc-IL-1ra-Fc, and ^{99m}Tc-TNFR2-Fc-IL-1ra obtained with a 2-IT/Protein ratio of 1000 are shown in Figure 2. Retention time on SEC-HPLC analysis was 12.5 minutes for ^{99m}Tc-IL-1ra-Fc, 10.6 minutes for ^{99m}Tc-TNFR-Fc, and 10.3 minutes for ^{99m}Tc-TNFR2-Fc-IL-1ra.

3.2. *In vitro* and *in vivo* stability

Stability tests using SEC-HPLC and paper chromatography showed no significant degradation of ^{99m}Tc-TNFR2-Rc-IL-1ra up to 6 hours in either saline at room temperature or serum at 37°C. After 6 hours, more than 94% of the radioactivity was still associated with each protein. At 21 hours, RCP was 90% in saline and 92.2% in serum. After challenge with cysteine to measure the degree of transchelation to the cysteine, the radioactivity bound to cytokine ligands was reduced from 99% to 91.1%, 74.3%, and 64.4% when using a ratio of protein to cysteine at 5, 100, and 500, respectively. As shown in Figure 3, SEC-HPLC analysis revealed one prominent peak of labeled ligand as well as radiolabeled species of lower molecular weight (Rt = 18.1) after cysteine challenge. These chromatographic results provided in vivo information that potential ^{99m}Tc activity from labeled cytokine ligand towards transchelation to cysteine.

The *in vivo* stability study with ^{99m}Tc-TNFR2-Fc-IL-1ra showed that 94.2% and 96.7% of the radioactivity in blood was associated with the plasma at 60 and 180 minutes post-injection, respectively, with the remaining amount associated with the cell fraction. HPLC analysis of plasma indicated that the radioactivity associated with injected radioligand was greater than 96% at 3 hours post-injection. There was no significant amount of free ^{99m}Tc present in the plasma.

3.3. Blood clearance and biodistribution measurements of ^{99m}Tc-labeled cytokine ligands

Results of blood radioactivity (%ID/g) and normalized clearance (% peak) of three cytokine radioligands over time, which were products with a ratio of 2IT to protein at 1000, are shown in Fig. 4. Administered specific activity (0,3 mL) was 4.6±0.2 for ^{99m}Tc-TNFR-Fc-IL-1ra, 4.3±0.2 for ^{99m}Tc-TNFR2-Fc, and 4.3±0.1 for ^{99m}Tc-IL-1ra-Fc. There was no

significant difference in the administered activity among three radioligands. After reaching an initial peak, the three radioligands exhibited continuous clearance over the observation period of 180 minutes post-injection. ^{99m}Tc fractional retention (% peak activity) at 180 minutes post-injection was 44.1 ± 0.6 for ^{99m}Tc-TNFR2-Fc-IL-1ra, 45.0 ± 1.6 for ^{99m}Tc-TNFR2-Fc, and 28.0 ± 2.5 for ^{99m}Tc-IL-1ra-Fc. There was no significant difference in fractional retention between ^{99m}Tc-TNFR2-Fc-IL-1ra and ^{99m}Tc-TNFR2-Fc. However, ^{99m}Tc-IL-1ra-Fc demonstrated faster washout and less retention than either ^{99m}Tc-TNFR2-Fc-IL-1ra or ^{99m}Tc-TNFR2-Fc. The exponential decay of the blood clearance curves in Figure 4 can be represented analytically by the following equations for (1) ^{99m}Tc-TNFR2-Fc-IL-1ra; (2) ^{99m}Tc-TNFR2-Fc; (3) ^{99m}Tc-IL-1ra-Fc:

$$A(t)=43.89+50.53 \times e^{-0.015t}, \gamma^2=0.969 \quad (1)$$

$$A(t)=40.19+55.86 \times e^{-0.013t}, \gamma^2=0.987 \quad (2)$$

$$A(t)=24.11+70.97 \times e^{-0.014t}, \gamma^2=0.986 \quad (3)$$

A(t) is radioactivity in normalized units at time (t) in minutes post-injection.

Tissue radioactivity distributions (%ID/g) in rats are summarized in Table 2. The organs with greatest activity at 180 minutes post-injection include liver, spleen, and kidneys. There was low radioactivity uptake in heart, skeletal muscle, and skin. Blood activity of ^{99m}Tc-IL-1ra-Fc was significantly lower than that of ^{99m}Tc-TNFR2-Fc-IL-1ra and ^{99m}Tc-TNFR2-Fc.

3.4. Uptake of ^{99m}Tc-labeled cytokine ligands in mouse TPA-induced ear edema model

Ear edema was observed in all animals that received TPA treatments. The results of ear thickness measurements are summarized in Table 3. The average thickness of right ears with TPA treatment increased significantly in comparison with initial thickness ($P < 0.01$). In the ears treated with vehicle, thickness remained unchanged ($P > 0.05$). Evidence of intense inflammatory reaction on histological examination was observed in the ears with TPA-induced edema. Representative microscopic images from a mouse ear with edema are shown in Figure 5. Subcutaneous edema along with heavy infiltration of inflammatory cells was observed in the TPA-treated ear but not in the control ear.

The inflamed ears in TPA-treated animals exhibited high accumulations of ^{99m}Tc-labeled cytokine ligands, which could be clearly detected by *in vivo* SPECT imaging, as shown in Figure 6. The radioactive uptake in the control ear was minimal and typically invisible by SPECT imaging. Less radioactive uptake of ^{99m}Tc-IL-1ra-Fc compared to ^{99m}Tc-TNFR2-Fc-IL-1ra and ^{99m}Tc-TNFR2-Fc was found in the inflamed ears. The *in vivo* specificity of inflammation targeting was established by blocking of radioactive uptake in the inflamed ears with non-radiolabeled IL-1ra-Fc or TNFR2-Fc/TNFR2-Fc-IL-1ra. Representative FastSPECT II and autoradiograph images of the ears in two mice with and without blockade are shown in Figure 7.

The activity (%ID/g) at 3 hours after injection in the inflamed ears and controls is summarized in Table 4. There was a significant difference in radioactive uptake between TPA-treated ears and control left ears for all three radioligands. The uptake level of ^{99m}Tc-TNFR2-Fc-IL-1ra in the inflamed ears was significantly higher than that of ^{99m}Tc-TNFR2-Fc and ^{99m}Tc-IL-1ra-Fc, and the uptake of ^{99m}Tc-TNFR2-Fc was significantly higher than that of ^{99m}Tc-IL-1ra-Fc. The average uptake of ^{99m}Tc-IL-1ra-Fc (%ID/g) in the control ears

was significantly lower than that of ^{99m}Tc-TNFR2-Fc-IL-1ra and ^{99m}Tc-TNFR2-Fc. ^{99m}Tc-TNFR2-Fc showed a tendency for greater accumulation in the control ears than ^{99m}Tc-TNFR2-Fc-IL-1ra, but it did not reach statistical significance.

The ratios of radioligand uptake in the inflamed and control ears were assessed. In order to eliminate contributions from carrier vehicle and nonspecific tissue activity, the activity measurements in the TPA-inflamed right ears were normalized using the measurements of the control left ears. After normalization, the ratios of TPA-inflamed ears to control ears were significantly higher for both ^{99m}Tc-TNFR2-Fc-IL-1ra and ^{99m}Tc-IL-1ra-Fc than for ^{99m}Tc-TNFR2-Fc ($P < 0.05$).

Blockade by the unlabeled ligand resulted in a significant decrease in radioactive uptake of ^{99m}Tc-IL-1ra-Fc, ^{99m}Tc-TNFR2-Fc, and ^{99m}Tc-TNFR2-Fc-IL-1ra in the inflamed ears, as shown in Table 4. A significant reduction of inflamed ear radioactivity was also evident on both *in vivo* images and *ex vivo* autoradiograph images after the blocking dose, as shown in Figure 6.

3.5. IL-1β and TNF-α expression in the inflamed mouse ears

Postmortem analysis of lysates prepared from mouse ears revealed that expression of IL-1β and TNFα was increased by TPA treatment. Immunoblot analyses of IL-lβ and IL-1RI using polyclonal antibodies are illustrated in Figure 8. Antibodies reacted strongly to IL-1β precursor and IL-1RI at the corresponding molecular weights 31 kilodaltons (kDa) and 80 kDa in the inflamed ear lysates, respectively. The band intensity of IL-1RI was much stronger than that of IL-1β. In the control ear lysates, IL-1β and IL-1RI were barely detectable. Moreover, the protein extracts reacted with the anti-TNF-α antibody at an apparent molecular weight of 26 kDa, which is consistent with membrane-bound TNF-α (Figure 8).

ELISA results of cytokine measurements in homogenized ear tissue are shown in Figure 9. The expression levels of IL-1β and TNFα (pg/ml) were significantly increased in TPA-inflamed ears compared with vehicle-treated ears. After normalization for total protein, IL-1β was 424.1 ± 14.9 pg/mg in the inflamed ears and 64.6 ± 20.9 pg/mg in the controls ($P < 0.05$). TNF-α in inflamed and control ears was 33.7 ± 4.2 pg/mg and 16.8 ± 1.3 pg/mg, respectively (P=0.013).

4. Discussion

The ability to obtain radiolabeled products with high efficiency, long stability, and unaltered cytokine binding capabilities is key to the future utilization of the IL-1 and TNF ligands. In this study, we investigated protocols for direct ^{99m}Tc-labeling of three recombinant cytokine ligands, TNFR2-Fc, IL-1ra-Fc, and TNFR2-Fc-IL-1ra, by addition of exogenous sulfhydryl groups with 2-iminothiolane (2-IT, Tram's reagent). This direct labeling employed a 2-step thiolation protocol that can be used effectively for small quantities of protein [27]. It involves the initial reduction of endogenous disulfide bonds to generate thiol binding sites. ^{99m}Tc can bind to the sulfur-containing amino acids in the proteins after reduction of the disulfide bonds [33]. We also evaluated the optimal molar ratio of 2-IT to protein for practical ^{99m}Tc labeling of small quantities of recombinant proteins and found that a ratio of 1000 resulted in high radiochemical purity without significant R/H ^{99m}Tc formation.

All radiolabeled preparations in this study showed good stability up to 6 hours in both saline and serum, with minor loss of radioactivity after 6 hours. It has been shown that directly labeled proteins are more susceptible to transchelation than indirectly labeled products [30, 34, 35]. In our studies, cysteine challenge at a 500-fold molar excess of cysteine showed

35.6% of translocation to cysteine, similar to other transchelation reports. However, our *in vivo* plasma data for ^{99m}Tc-TNFR2-Fc-IL-1ra showed greater than 96% retention of radioactivity at 3 hours post-injection. Although it is possible that some *in vivo* transchelation may take place in tissue, no significant amount of translocation to cysteine in the plasma was observed in this study.

The development of a successful cytokine radioligand for SPECT imaging of inflammation requires a number of different criteria to be met. Ideally, the radioligand should be rapidly cleared from the circulation to allow for sufficient contrast between inflammatory lesions and normal surrounding tissues and blood pool. In comparison with indirect labeling, as described in the literature and in our pilot studies, direct labeling yields radioligands with more rapid blood clearance and lower liver uptake [35]. We have also implemented an indirect labeling approach using 6-hydrazinopyridine-3-carboxylic acid (HYNIC) as a bifunctional chelator (data not shown). When we radiolabeled TNFR2-Fc with ^{99m}Tc through HYNIC conjugation, we found that ^{99m}Tc-TNFR2-Fc remained in the bloodstream and had very limited tissue distribution within 3 hours post-injection. When we directly labeled TNFR2-Fc using 2-IT thiolation, the blood clearance of ^{99m}Tc-TNFR2-Fc improved significantly.

In the present study, ^{99m}Tc-IL-1ra-Fc showed the fastest blood clearance compared to ^{99m}Tc-TNFR2-Fc and ^{99m}Tc-TNFR2-Fc-IL-1ra. ^{99m}Tc-TNFR2-Fc-IL-1ra exhibited a pharmacokinetic profile very similar to that of ^{99m}Tc-TNFR2-Fc, even though TNFR2-Fc-IL-1ra has a larger molecular size (165 kDa) than TNFR2-Fc (150 kDa). It is possible that IL-1ra may enhance the blood clearance of its fusion protein.

In an effort to determine whether radiolabeled cytokine ligands target inflammation *in vivo*, we used a TPA-induced ear edema inflammation model for imaging studies. TPA-induced skin inflammation is a well-established model for investigating cytokine targeting of inflammation since it is characterized by high production of cytokines, including IL-1β, IL-6, IL-12, and TNF-α [36, 37]. IL-1β and TNF-α mediate inflammatory signaling and play a pivotal role in TPA-induced acute irritant contact dermatitis [38–42]. Our study showed that TPA exposure resulted in significant local increase in the tissue level of IL-1β, the prototypical cytokine with pleiotropic effects. The IL-1β pathway plays a major rule in mediating transcription of adhesion molecules, chemokines, secondary cytokines, nitric oxide synthase, and cyclooxygenase, all relevant to skin inflammation. Western blot analysis in our TPA-induced ear edema model showed dramatically upregulated local expression of IL-1RI, which was more significant compared to the increase of IL-1β and correlated to the site-directed high uptake of ^{99m}Tc-IL-1ra and ^{99m}Tc-TNFR2-Fc-IL-1ra.

The skin edema induced by TPA was accompanied by an increase in the level of TNF-α at the inflamed site. The involvement of TNF-α has been widely validated in many inflammation and anti-inflammatory studies [25, 32, 37, 43–45]. TNF-α-deficient mice fail to develop skin inflammation following the topical application of TPA to their ears [45]. TPA-induced ear edema provides a simple and efficient animal model for inflammation imaging studies based on the TNF-α pathway. However, ELISA analysis in the present study showed that expression of TNF-α in the inflamed ears was only 2.1-fold higher than in the control ears. The increase of TNF-α was not as great as the increase of IL-1β, which was 11.4-fold higher in the TPA-treated ears compared to controls. In one prior report the increase of TNF-α peaked at 5 hours following the application [46]. In the present study, the cytokine targeting studies were performed 24 hours post-TPA treatment. The animals were subsequently euthanized 3 hours after cytokine radioligand injection for postmortem analysis and cytokine measurements. Thus, the peak time for TPA-stimulated TNF-α expression might have passed.

An ideal radioligand for scintigraphic imaging of inflammation should bind specifically to inflammatory components with high affinity and sufficient residence time at the inflammatory sites to allow for optimal imaging. Our experimental results indicate that ^{99m}Tc-TNFR2-Fc, ^{99m}Tc-IL-1ra-Fc, and ^{99m}Tc-TNFR2-Fc-IL-1ra may all be capable of specific inflammation imaging, as demonstrated by the blocking experiments with unlabeled ligands. The blockades did not reduce the radioactivity in the remote normal ears, which indicated that the radioactive accumulations were not through a specific binding mechanism. We found that the dual-domain ^{99m}Tc-TNFR2-Fc-IL-1ra had greater uptake in inflammatory sites than the two individual radioligands. However, it is not yet clear whether the increased uptake of ^{99m}Tc-TNFR2-Fc-IL-1ra is mainly due to the high expression of IL-1 receptors or TNF-α. As shown in Figure 1, TNF-α exists in two forms, a precursor 26-kDa membrane-bound form (mTNF) on TNF-producing cells and a 17-kDa soluble form (sTNF) in the context of tissues, both of which are bioactive [47, 48]. In principle, sTNF and mTNF are biological targets for ^{99m}Tc-TNFR2-Fc and TNFR2-domain of ^{99m}Tc-TNFR2-Fc-IL-1ra. The targets of ^{99m}Tc-IL-1ra-Fc and IL-1ra domain of ^{99m}Tc-TNFR2-Fc-IL-1ra are IL-1 receptors. When the TNFR2 domain of ^{99m}Tc-TNFR2-Fc-IL-1ra biologically binds to sTNF or mTNF, the IL-1ra domain is expected to be capable to bind to IL-1 receptor on other cell membrane. There would be competition between natural IL-1 and ^{99m}Tc-IL-1ra-Fc or the IL-1ra domain of ^{99m}Tc-TNFR2-Fc-IL-1ra if there was only a limited number of IL-1 receptor. The results of our Western blot analysis indicated that IL-1β and IL-1RI were both overexpressed in the inflamed ears compared to that in the controlled ears. IL-1RI was upregulated about 15-fold higher than IL-1β. Thus, the overall uptake of ^{99m}Tc-IL-1ra-Fc or ^{99m}Tc-TNFR2-Fc-IL-1ra was increased significantly.

It should be noted that increased capillary permeability at sites of inflammation always contributes to accumulation of radiolabeled large molecules. As a result, the radioactivity detected in the inflamed ear lesions might be a combination of specific cytokine binding and nonspecific leakage of the cytokine ligands. The contribution of nonspecific leakage in the inflamed lesions might be more significant for ^{99m}Tc-TNFR2-Fc-IL-1ra and ^{99m}Tc-TNFR2-Fc because of their higher blood retention. The contribution of nonspecific binding and leakage needs to be quantitatively clarified in further studies using radiolabeled non-specific antibodies or proteins with similar molecular weight.

Molecular imaging using the dual-domain cytokine radioligand in this study holds promise for specific detection of inflammation via IL-1 and TNF pathways, as these two pro-inflammatory cytokines mediate a large group of disorders. Specifically, ^{99m}Tc-TNFR2-Fc-IL-1ra may have some advantages over the individual radioligands, including specificity, high affinity, and better radiopharmaceutical kinetics. The carboxy-terminal sequence of ^{99m}Tc-TNFR2-Fc-IL-1ra may act as a competitive receptor antagonist for binding of IL-1 to membrane-bound IL-1RI in numerous cell types. The amino-terminal segment of ^{99m}Tc-TNFR2-Fc-IL-1ra may specifically bind to TNF-α and function independently. When ^{99m}Tc-TNFR2-Fc-IL-1ra is bound to IL-1RI on the cell surface in inflammatory tissues, the TNFR2 domain may retain the ability to bind TNF-α. Theoretically, when ^{99m}Tc-TNFR2-Fc-IL-1ra is systemically administered, the TNFR2 domain can target circulating TNF-α. However, because exogenous IL-1ra exhibits rapid blood clearance in humans and other species [49–51], the recombinant IL-1ra domain may quickly guide ^{99m}Tc-TNFR2-Fc-IL-1ra to IL-1 receptor-rich inflammatory sites.

Unlike conventional imaging methods that rely on anatomical, physiological or metabolic changes to provide an indirect or non-specific demonstration of inflammation [53–55], specific inflammation imaging by interrogation of the inflammatory response and cytokine pathways offers an opportunity to noninvasively detect inflammation and promote timely therapeutic intervention. ^{99m}Tc-TNFR2-Fc-IL-1ra SPECT imaging may provide an efficient

tool for targeting inflammatory components and guiding therapy in diseases such as arthritis, ankylosing spondylitis, inflammatory bowel disease, psoriasis, sarcoidosis, and cardiovascular diseases [21, 56]. For example, we have found that ^{99m}Tc-TNFR2-Fc-IL-1ra exhibited more potent affinity with enhanced uptake in the inflammatory sites of ischemic-reperfused hearts compared to the single-domain ligands (data not published). We are investigating whether the upregulated uptake of ^{99m}Tc-TNFR2-Fc-IL-1ra is a sensitive indicator of the expansion of myocyte injury associated with the inflammatory reaction of ischemia-reperfusion injury, in which the involvement of cytokines is a cascade event related to IL-1β and TNF-α [57–59]. ^{99m}Tc-ILTNFR2-Fc-IL-1ra may also be used to evaluate the inflammation accompanying other cardiovascular disorders such as atherosclerosis, cardiomyopathy, and myocarditis. In atherosclerosis, the intense inflammatory response following cholesterol buildup has been implicated as a critical factor in atherosclerosis destabilization and plaque rupture, which induces stroke and acute coronary events (ACE). IL-1β and TNF-α are both potent pro-inflammatory cytokines involved in initiating and accelerating progression of atherosclerotic plaques. High-resolution SPECT imaging with ^{99m}Tc-ILTNFR2-Fc-IL-1ra may enable detection of plaque sites, extent and vulnerability before ACE to permit a stratified approach to therapy. In rheumatoid arthritis, a plethora of pro-inflammatory cytokines, including TNF-α, IL-1, IL-6, IL-7, IL-17, IL-18, and interferon-γ are involved in synovial inflammation and the resulting joint destruction and cartilage degradation [56, 60]. The production of TNF-α and IL-1 in the synovial membrane correlates significantly with local inflammation [61]. A variety of cytokine-based strategies are being explored for treating patients with rheumatoid arthritis, including use of recombinant human IL-1ra (anakinra) and TNFR2-Fc (etanercept), as noted previously [6]. An objective approach is needed to evaluate treatment response and disease activity, because the presentation of the disease may vary considerably [56]. Targeting IL-1β and TNF-α (and possibly other cytokines) using cytokine radioligands may also have a significant clinical impact on prognosis and stratification in individual patients [21].

5. Conclusions

Three cytokine ligands were successfully radiolabeled with ^{99m}Tc via 2-iminothiolane thiolation. ^{99m}Tc-TNFR2-Fc, ^{99m}Tc-IL-1ra-Fc, and ^{99m}Tc-TNFR2-Fc-IL-1ra appear to provide specific approaches for assessment of inflammation and inflammatory response. The dual-domain fusion protein, ^{99m}Tc-TNFR2-Fc-IL-1ra, may hold advantages in inflammation imaging since it has more potent affinity and enhanced uptake in inflammatory sites compared to the single-domain ligands.

Acknowledgments

The authors are grateful to Dr. Gail Stevenson for support in animal protocol preparation, amendment, and animal studies, and to April Lake for assistance in Western blot analysis. We wish to thank Dr. Paul McDonagh for allowing use of his laboratory materials and equipment in tissue processing. Dr. Mizhou Hui is the owner of AmProtein Inc. This work was supported by NIH grants NHLBI R01-HL090716 and NIBIB P41-EB002035.

References

1. Dinarello CA. Biologic basis for interleukin-1 in disease. Blood. 1996; 87:2095–2147. [PubMed: 8630372]
2. Dinarello CA. Interleukin 1 and interleukin 18 as mediators of inflammation and the aging process. Am J Clin Nutr. 2006; 83:447S–455S. [PubMed: 16470011]
3. Eisenberg SP, Evans RJ, Arend WP, Verderber E, Brewer MT, Hannum CH, et al. Primary structure and functional expression from complementary DNA of a human interleukin-1 receptor antagonist. Nature. 1990; 343:341–346. [PubMed: 2137201]

4. Bresnihan B. The prospect of treating rheumatoid arthritis with recombinant human interleukin-1 receptor antagonist. BioDrugs. 2001; 15:87–97. [PubMed: 11437678]
5. Efthimiou P, Markenson JA. Role of biological agents in immune-mediated inflammatory diseases. South Med J. 2005; 98:192–204. [PubMed: 15759950]
6. Thompson RC, Dripps DJ, Eisenberg SP. Interleukin-1 receptor antagonist (IL-1ra) as a probe and as a treatment for IL-1 mediated disease. Int J Immunopharmacol. 1992; 14:475–480. [PubMed: 1535616]
7. Lewis AM, Varghese S, Xu H, Alexander HR. Interleukin-1 and cancer progression: the emerging role of interleukin-1 receptor antagonist as a novel therapeutic agent in cancer treatment. J Transl Med. 2006; 4:48. [PubMed: 17096856]
8. Vilcek J, Lee TH. Tumor necrosis factor. New insights into the molecular mechanisms of its multiple actions. J Biol Chem. 1991; 266:7313–7316. [PubMed: 1850405]
9. Van Zee KJ, Kohno T, Fischer E, Rock CS, Moldawer LL, Lowry SF. Tumor necrosis factor soluble receptors circulate during experimental and clinical inflammation and can protect against excessive tumor necrosis factor alpha in vitro and in vivo. Proc Natl Acad Sci U S A. 1992; 89:4845–4849. [PubMed: 1317575]
10. Fernandez-Botran R. Soluble cytokine receptors: novel immunotherapeutic agents. Expert Opin Investig Drugs. 2000; 9:497–514.
11. Fernandez-Botran R, Crespo FA, Sun X. Soluble cytokine receptors in biological therapy. Expert Opin Biol Ther. 2002; 2:585–605. [PubMed: 12171504]
12. Cain BS, Meldrum DR, Dinarello CA, Meng X, Joo KS, Banerjee A, et al. Tumor necrosis factor-alpha and interleukin-1beta synergistically depress human myocardial function. Crit Care Med. 1999; 27:1309–1318. [PubMed: 10446825]
13. Horton WE Jr, Udo I, Precht P, Balakir R, Hasty K. Cytokine inducible matrix metalloproteinase expression in immortalized rat chondrocytes is independent of nitric oxide stimulation. In Vitro Cell Dev Biol Anim. 1998; 34:378–384. [PubMed: 9639100]
14. Di Girolamo N, Lloyd A, McCluskey P, Filipic M, Wakefield D. Increased expression of matrix metalloproteinases in vivo in scleritis tissue and in vitro in cultured human scleral fibroblasts. Am J Pathol. 1997; 150:653–666. [PubMed: 9033278]
15. Dinarello CA. Novel targets for interleukin 18 binding protein. Ann Rheum Dis. 2001; 60(Suppl 3):iii18–iii24. [PubMed: 11890646]
16. Woldbaek PR, Tonnessen T, Henriksen UL, Florholmen G, Lunde PK, Lyberg T, et al. Increased cardiac IL-18 mRNA, pro-IL-18 and plasma IL-18 after myocardial infarction in the mouse; a potential role in cardiac dysfunction. Cardiovasc Res. 2003; 59:122–131. [PubMed: 12829183]
17. Kan H, Xie Z, Finkel MS. TNF-alpha enhances cardiac myocyte NO production through MAP kinase-mediated NF-kappaB activation. Am J Physiol. 1999; 277:H1641–H1646. [PubMed: 10516205]
18. Kuiper S, Joosten LA, Bendele AM, Edwards CK 3rd, Arntz OJ, Helsen MM, et al. Different roles of tumour necrosis factor alpha and interleukin 1 in murine streptococcal cell wall arthritis. Cytokine. 1998; 10:690–702. [PubMed: 9770330]
19. Bendele AM, Chlipala ES, Scherrer J, Frazier J, Sennello G, Rich WJ, et al. Combination benefit of treatment with the cytokine inhibitors interleukin-1 receptor antagonist and PEGylated soluble tumor necrosis factor receptor type I in animal models of rheumatoid arthritis. Arthritis and rheumatism. 2000; 43:2648–2659. [PubMed: 11145022]
20. Feige U, Hu YL, Gasser J, Campagnuolo G, Munyakazi L, Bolon B. Anti-interleukin-1 and anti-tumor necrosis factor-alpha synergistically inhibit adjuvant arthritis in Lewis rats. Cellular and molecular life sciences : CMLS. 2000; 57:1457–1470. [PubMed: 11078023]
21. Glaudemans AW, Dierckx RA, Kallenberg CG, Anzola Fuentes KL. The role of radiolabelled anti-TNFa monoclonal antibodies for diagnostic purposes and therapy evaluation. Q J Nucl Med Mol Imaging. 2010; 54:639–653. [PubMed: 21221071]
22. Goldenberg MM. Etanercept, a novel drug for the treatment of patients with severe, active rheumatoid arthritis. Clinical therapeutics. 1999; 21:75–87. discussion 71–72. [PubMed: 10090426]

23. Bitonti AJ, Dumont JA, Low SC, Peters RT, Kropp KE, Palombella VJ, et al. Pulmonary delivery of an erythropoietin Fc fusion protein in non-human primates through an immunoglobulin transport pathway. Proc Natl Acad Sci U S A. 2004; 101:9763–9768. [PubMed: 15210944]
24. Goffe B. Etanercept (Enbrel) -- an update. Skin therapy letter. 2004; 9:1–4. 9. [PubMed: 15657632]
25. Cao Q, Cai W, Li ZB, Chen K, He L, Li HC, et al. PET imaging of acute and chronic inflammation in living mice. Eur J Nucl Med Mol Imaging. 2007; 34:1832–1842. [PubMed: 17541586]
26. Liu Z, wyffels L, Barber C, Hui MM, Woolfenden JM. A ^{99m}Tc-labeled dual-domain cytokine ligand for imaging of inflammation. Nucl Med Biol. 2011; 38:795–805. [PubMed: 21843776]
27. Tesic M, Sheldon KM, Ballinger JR, Boxen I. Labelling small quantities of monoclonal antibodies and their F(ab')2 fragments with technetium-99m. Nucl Med Biol. 1995; 22:451–457. [PubMed: 7550021]
28. Zhao M, Zhu X, Ji S, Zhou J, Ozker KS, Fang W, et al. ^{99m}Tc-labeled C2A domain of synaptotagmin I as a target-specific molecular probe for noninvasive imaging of acute myocardial infarction. J Nucl Med. 2006; 47:1367–1374. [PubMed: 16883018]
29. Mishra AK, Iznaga-Escobar N, Figueredo R, Jain VK, Dwarakanath BS, Perez-Rodriguez R, et al. Preparation and comparative evaluation of ^{99m}Tc-labeled 2-iminothiolane modified antibodies and CITC-DTPA immunoconjugates of anti-EGF-receptor antibodies. Methods Find Exp Clin Pharmacol. 2002; 24:653–660. [PubMed: 12616957]
30. Hnatowich DJ, Virzi F, Fogarasi M, Rusckowski M, Winnard P Jr. Can a cysteine challenge assay predict the in vivo behavior of 99mTc-labeled antibodies? Nucl Med Biol. 1994; 21:1035–1044. [PubMed: 9234361]
31. Kim EJ, Park H, Kim J, Park JH. 3,3'-diindolylmethane suppresses 12-O-tetradecanoylphorbol-13-acetate-induced inflammation and tumor promotion in mouse skin via the downregulation of inflammatory mediators. Mol Carcinog. 2010; 49:672–683. [PubMed: 20564344]
32. Updyke LW, Yoon HL, Chuthaputti A, Pfeifer RW, Yim GK. Induction of interleukin-1 and tumor necrosis factor by 12-O-tetradecanoylphorbol-13-acetate in phorbol ester-sensitive (SENCAR) and resistant (B6C3F1) mice. Carcinogenesis. 1989; 10:1107–1111. [PubMed: 2785869]
33. Hnatowich DJ. Recent developments in the radiolabeling of antibodies with iodine, indium, and technetium. Seminars in nuclear medicine. 1990; 20:80–91. [PubMed: 2404343]
34. Viaggi MEC J, de Castiglia SG. In vitro and in vivo studies of ^{99m}Tc IgG: A comparison between three labeling methods. J. Radioanal. Nucl. Chem. 1999; 241:173–177.
35. Hnatowich DJ, Mardirossian G, Rusckowski M, Fogarasi M, Virzi F, Winnard P Jr. Directly and indirectly technetium-99m-labeled antibodies--a comparison of in vitro and animal in vivo properties. Journal of nuclear medicine : official publication, Society of Nuclear Medicine. 1993; 34:109–119.
36. Teige I, Hvid H, Svensson L, Kvist PH, Kemp K. Regulatory T cells control VEGF-dependent skin inflammation. J Invest Dermatol. 2009; 129:1437–1445. [PubMed: 19037231]
37. Hvid H, Teige I, Kvist PH, Svensson L, Kemp K. TPA induction leads to a Th17-like response in transgenic K14/VEGF mice: a novel in vivo screening model of psoriasis. Int Immunol. 2008; 20:1097–1106. [PubMed: 18579711]
38. Kalyan Kumar G, Dhamotharan R, Kulkarni NM, Mahat MY, Gunasekaran J, Ashfaque M. Embelin reduces cutaneous TNF-alpha level and ameliorates skin edema in acute and chronic model of skin inflammation in mice. Eur J Pharmacol. 2011; 662:63–69. [PubMed: 21549694]
39. Lilleholt LL, Johansen C, Arthur JS, Funding A, Bibby BM, Kragballe K, et al. Role of p38 mitogen-activated protein kinase isoforms in murine skin inflammation induced by 12-O-tetradecanoylphorbol 13-acetate. Acta dermato-venereologica. 2011; 91:271–278. [PubMed: 21336470]
40. Choi SP, Kim SP, Kang MY, Nam SH, Friedman M. Protective effects of black rice bran against chemically-induced inflammation of mouse skin. Journal of agricultural and food chemistry. 2010; 58:10007–10015. [PubMed: 20731354]
41. Song HY, Lee JA, Ju SM, Yoo KY, Won MH, Kwon HJ, et al. Topical transduction of superoxide dismutase mediated by HIV-1 Tat protein transduction domain ameliorates 12-O-

tetradecanoylphorbol-13-acetate (TPA)-induced inflammation in mice. Biochemical pharmacology. 2008; 75:1348–1357. [PubMed: 18164693]

42. Otuki MF, Vieira-Lima F, Malheiros A, Yunes RA, Calixto JB. Topical antiinflammatory effects of the ether extract from Protium kleinii and alpha-amyrin pentacyclic triterpene. Eur J Pharmacol. 2005; 507:253–259. [PubMed: 15659316]
43. Murakawa M, Yamaoka K, Tanaka Y, Fukuda Y. Involvement of tumor necrosis factor (TNF)-alpha in phorbol ester 12-O-tetradecanoylphorbol-13-acetate (TPA)-induced skin edema in mice. Biochem Pharmacol. 2006; 71:1331–1336. [PubMed: 16487490]
44. Robertson FM, Ross MS, Tober KL, Long BW, Oberyszyn TM. Inhibition of pro-inflammatory cytokine gene expression and papilloma growth during murine multistage carcinogenesis by pentoxifylline. Carcinogenesis. 1996; 17:1719–1728. [PubMed: 8761432]
45. Moore RJ, Owens DM, Stamp G, Arnott C, Burke F, East N, et al. Mice deficient in tumor necrosis factor-alpha are resistant to skin carcinogenesis. Nat Med. 1999; 5:828–831. [PubMed: 10395330]
46. Murakawa M, Yamaoka K, Tanaka Y, Fukuda Y. Involvement of tumor necrosis factor (TNF)-alpha in phorbol ester 12-O-tetradecanoylphorbol-13-acetate (TPA)-induced skin edema in mice. Biochemical pharmacology. 2006; 71:1331–1336. [PubMed: 16487490]
47. Wallach D, Engelmann H, Nophar Y, Aderka D, Kemper O, Hornik V, et al. Soluble and cell surface receptors for tumor necrosis factor. Agents and actions. Supplements. 1991; 35:51–57. [PubMed: 1664189]
48. Kriegler M, Perez C, DeFay K, Albert I, Lu SD. A novel form of TNF/cachectin is a cell surface cytotoxic transmembrane protein: ramifications for the complex physiology of TNF. Cell. 1988; 53:45–53. [PubMed: 3349526]
49. Barrera P, van der Laken CJ, Boerman OC, Oyen WJ, van de Ven MT, van Lent PL, et al. Radiolabelled interleukin-1 receptor antagonist for detection of synovitis in patients with rheumatoid arthritis. Rheumatology (Oxford). 2000; 39:870–874. [PubMed: 10952741]
50. Granowitz EV, Porat R, Mier JW, Pribble JP, Stiles DM, Bloedow DC, et al. Pharmacokinetics, safety and immunomodulatory effects of human recombinant interleukin-1 receptor antagonist in healthy humans. Cytokine. 1992; 4:353–360. [PubMed: 1420996]
51. van der Laken CJ, Boerman OC, Oyen WJ, van de Ven MT, Claessens RA, van der Meer JW, et al. Different behaviour of radioiodinated human recombinant interleukin-1 and its receptor antagonist in an animal model of infection. Eur J Nucl Med. 1996; 23:1531–1535. [PubMed: 8854854]
52. Vassalli P. The pathophysiology of tumor necrosis factors. Annual review of immunology. 1992; 10:411–452.
53. Jalilian AR, Bineshmarvasti M, Sardari S. Application of radioisotopes in inflammation. Curr Med Chem. 2006; 13:959–965. [PubMed: 16611077]
54. Villanueva FS, Wagner WR, Vannan MA, Narula J. Targeted ultrasound imaging using microbubbles. Cardiol Clin. 2004; 22:283–298. vii. [PubMed: 15158940]
55. Jaffer FA, Weissleder R. Seeing within: molecular imaging of the cardiovascular system. Circ Res. 2004; 94:433–445. [PubMed: 15001542]
56. Gotthardt M, Bleeker-Rovers CP, Boerman OC, Oyen WJ. Imaging of inflammation by PET, conventional scintigraphy, and other imaging techniques. J Nucl Med. 2010; 51:1937–1949. [PubMed: 21078798]
57. Nian M, Lee P, Khaper N, Liu P. Inflammatory cytokines and postmyocardial infarction remodeling. Circ Res. 2004; 94:1543–1553. [PubMed: 15217919]
58. Ren G, Dewald O, Frangogiannis NG. Inflammatory mechanisms in myocardial infarction. Curr Drug Targets Inflamm Allergy. 2003; 2:242–256. [PubMed: 14561159]
59. Roy S, Khanna S, Kuhn DE, Rink C, Williams WT, Zweier JL, et al. Transcriptome analysis of the ischemia-reperfused remodeling myocardium: temporal changes in inflammation and extracellular matrix. Physiol Genomics. 2006; 25:364–374. [PubMed: 16554547]
60. Malemud CJ. Anticytokine therapy for osteoarthritis: evidence to date. Drugs Aging. 2010; 27:95–115. [PubMed: 20104937]
61. Joosten LA, Radstake TR, Lubberts E, van den Bersselaar LA, van Riel PL, van Lent PL, et al. Association of interleukin-18 expression with enhanced levels of both interleukin-1beta and tumor

necrosis factor alpha in knee synovial tissue of patients with rheumatoid arthritis. Arthritis Rheum. 2003; 48:339–347. [PubMed: 12571842]

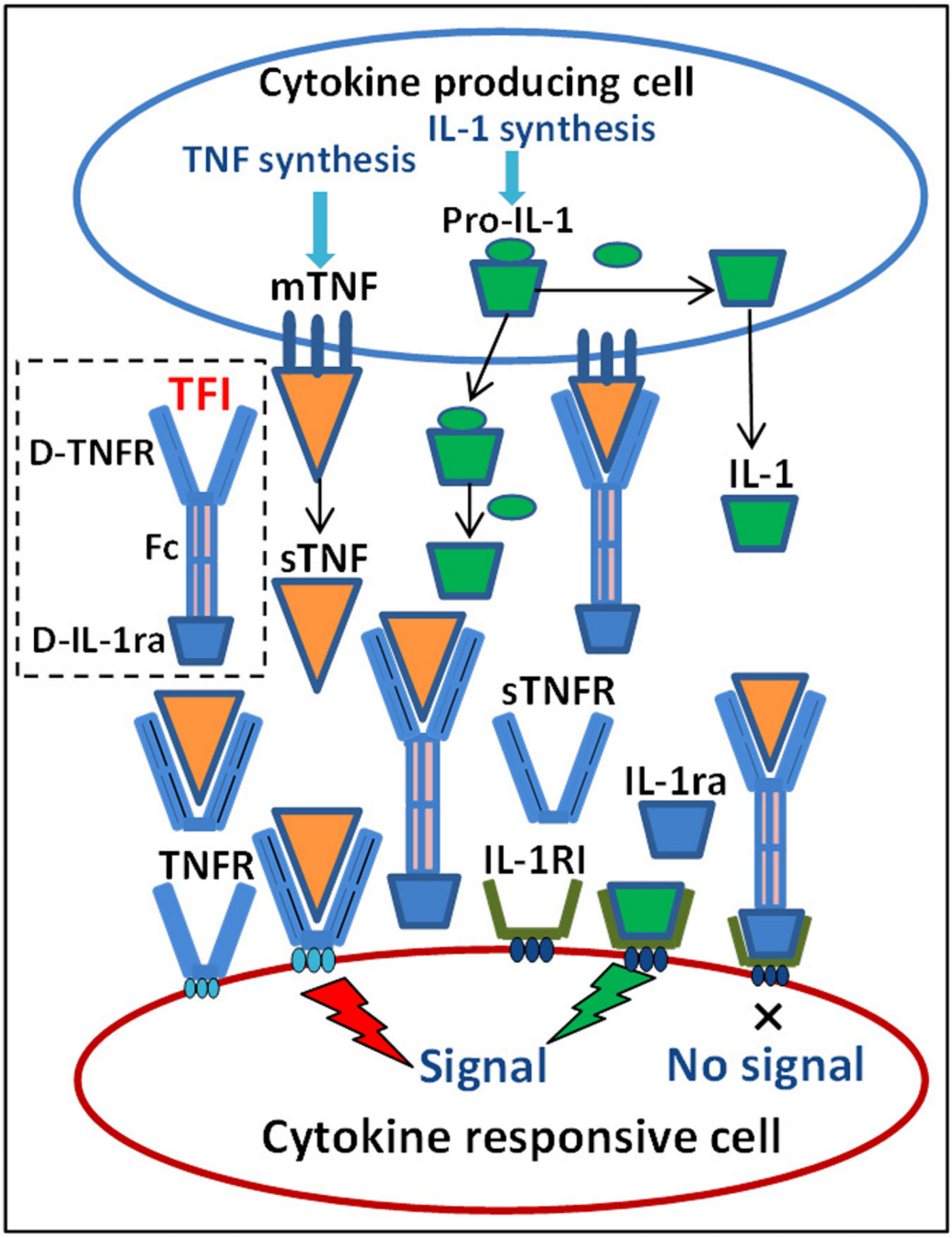

Figure 1.

Schematic representation of TNF and IL-1 receptors, ligands, interactions, and ^{99m}Tc-TNFR2-Fc-IL-1ra binding mechanism. IL-1: interleukin 1; Pro-IL-1: IL-1 precursor; IL-1RI: type I IL-1 receptor; mTNF: membrane-bound tumor necrosis factor; sTNF: soluble TNF; TNFR: TNF receptor; sTNFR: soluble TNFR; TFI: ^{99m}Tc-TNFR2-Fc-IL-1ra; D-TNFR: TNFR2 domain of TFI; D-IL-1ra: IL-1ra domain of TFI.

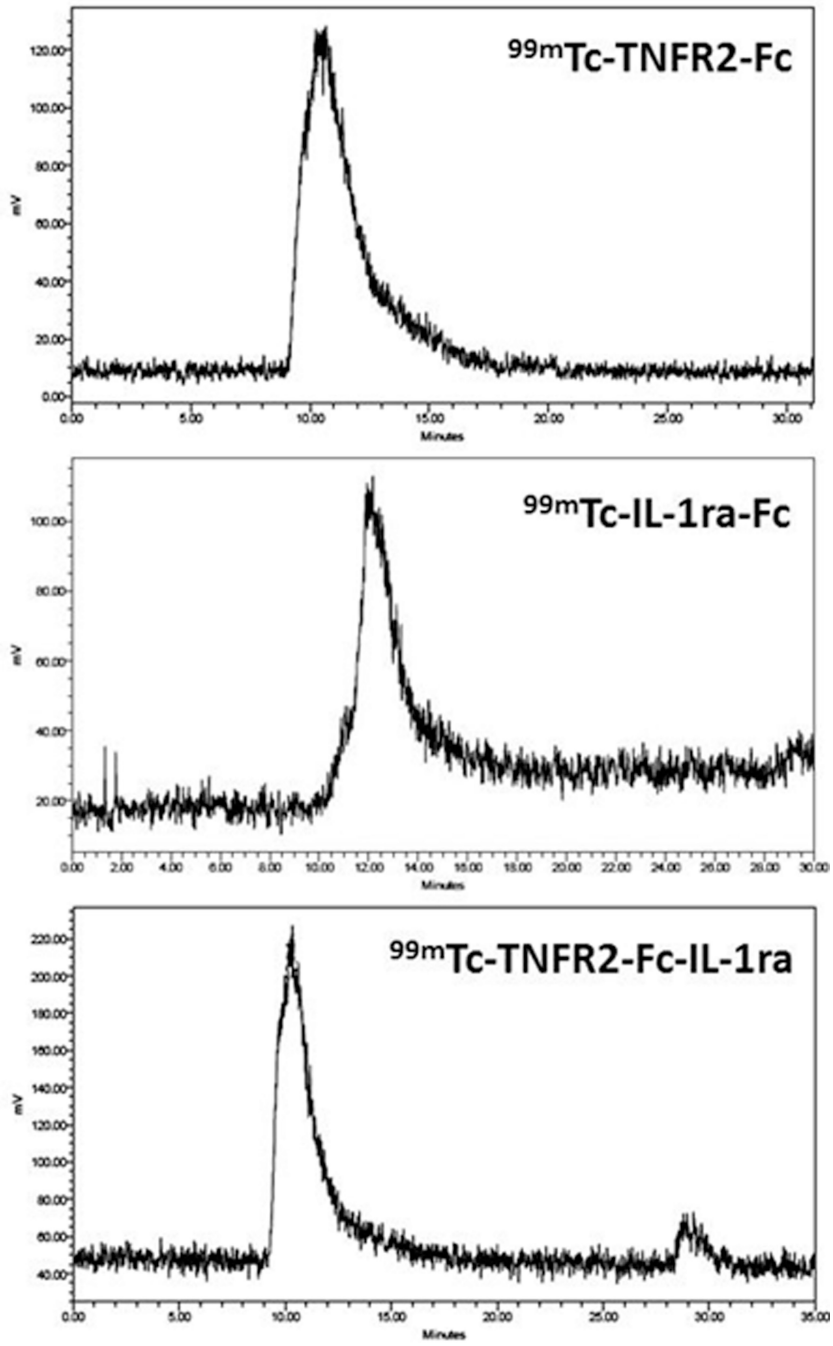

Figure 2.

Representative HPLC-chromatograms of ^{99m}Tc-labeled TNFR2-Fc (Top), IL-1ra-Fc (middle), and TNFR2-Fc-IL-1ra (bottom) following a 2-step thiolation protocol with 2IT/protein molar ratio of 1000:1 prior to gel purification.

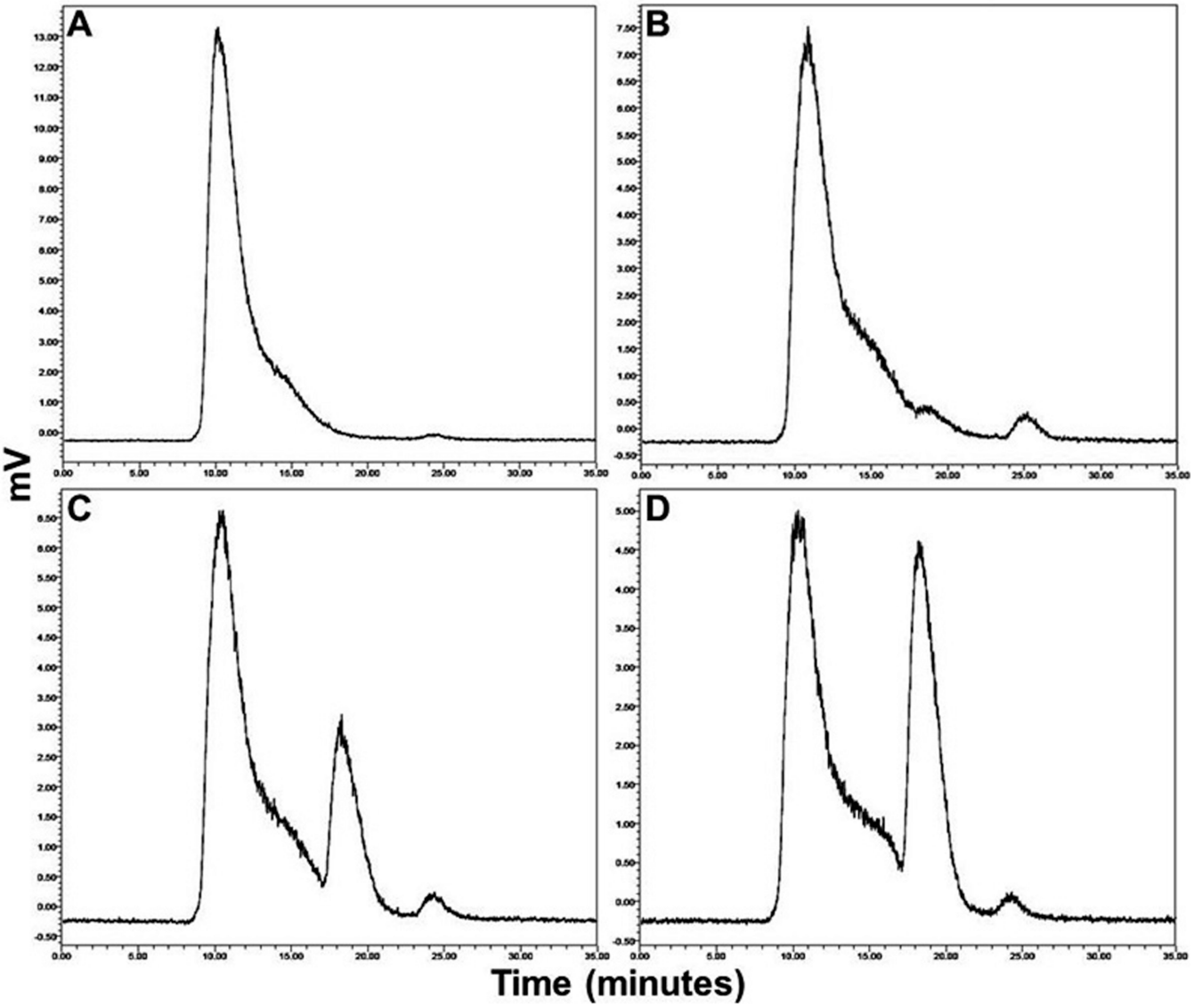

Figure 3.

Representative HPLC-chromatograms of ^{99m}Tc-TNFR2-Fc-IL-1ra in cysteine challenge testing after incubating the purified ^{99m}Tc-labeled protein with cysteine hydrochloride at a cysteine/protein molar ratio of 0 (A), 5 (B), 100 (C), and 500 (D) in phosphate buffer for 1 hour at 37°C.

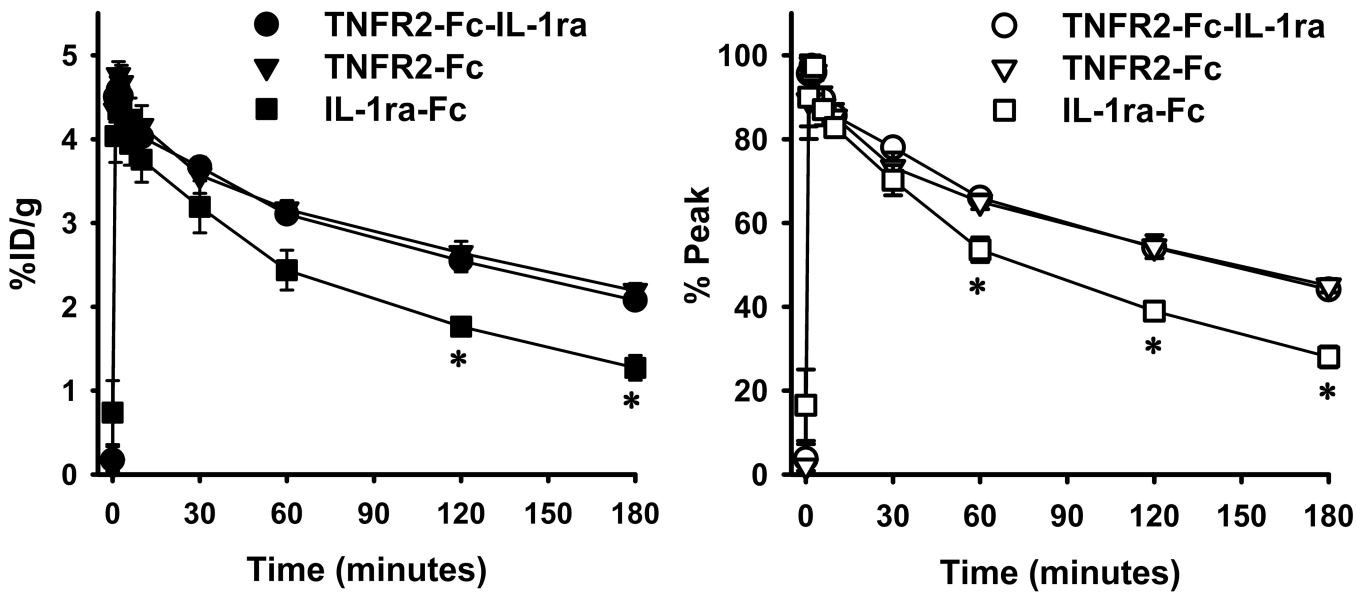

Figure 4.

Blood-clearance curves of ^{99m}Tc-labeled cytokine ligands in healthy rats. Left panel: Original blood-clearance data in terms of %ID/g; Right panel: Normalized blood-clearance curves, in which radioactivity at each time point is given as percentage of peak activity at 2 minutes post-injection.

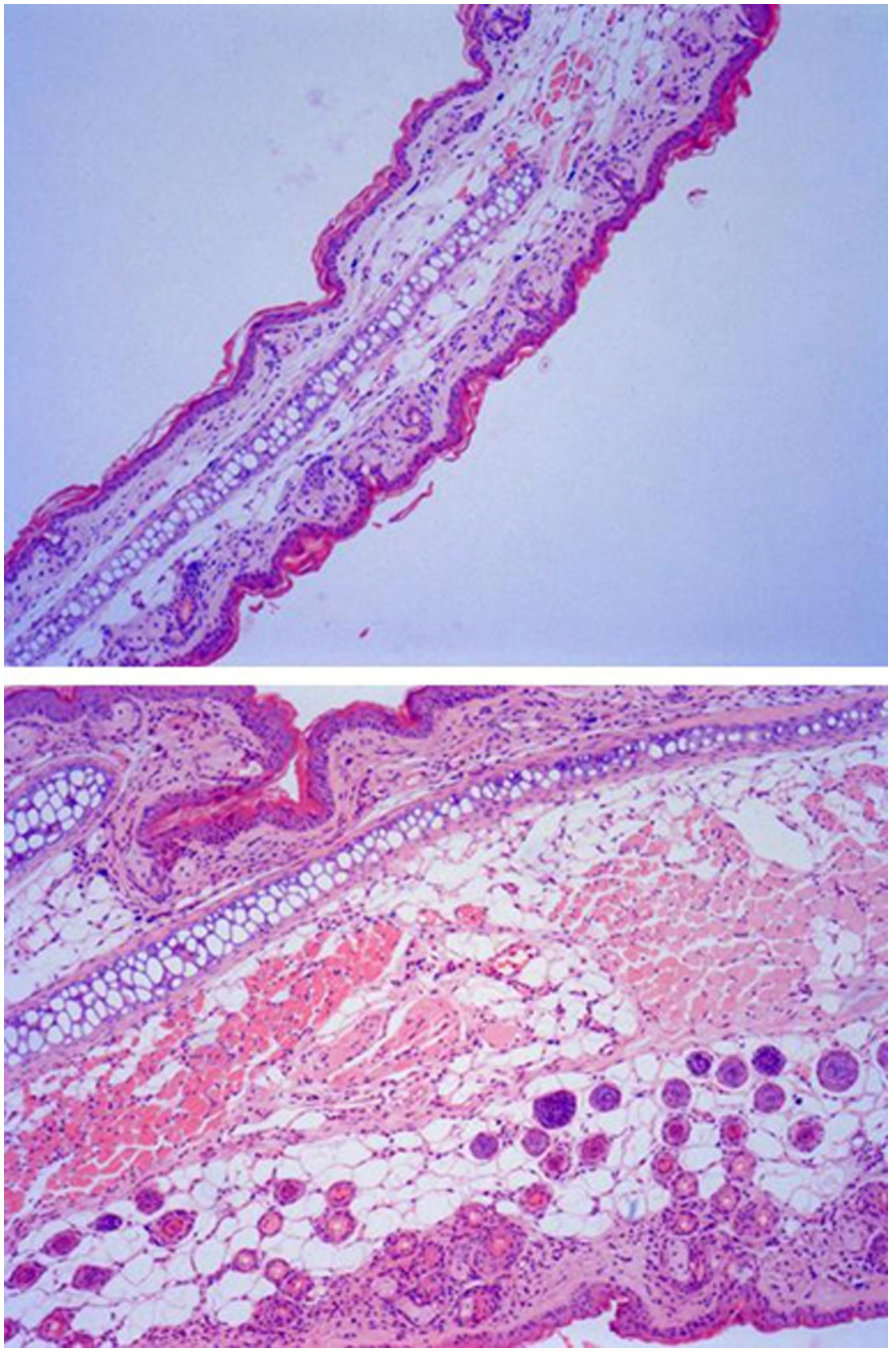

Figure 5.
Hematoxylin and eosin (H&E) stained histological sections of mouse ears treated with carrier vehicle (upper panel, 10 μm) and TPA (lower panel, 10 μm). TPA treatment induced a significant increase in ear thickness accompanied by the characteristic histological features of edema and inflammatory cell infiltration.

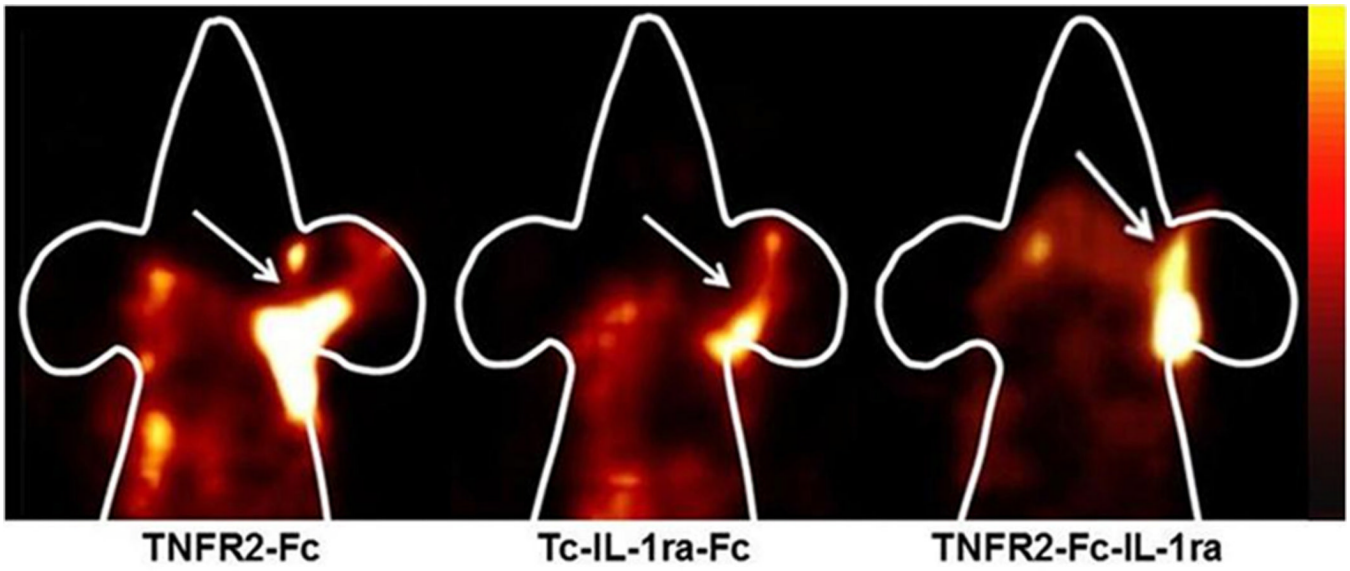

Figure 6.

Representative SPECT images in mice with TPA-induced right ear edema and acetone-treated left ear control. The SPECT images were acquired for 10 minutes at 3 hours post-injection of 3.5–4.5 mCi (0.2 ml) ^{99m}Tc-labeled cytokine ligands. The animals were anesthetized with 1.5% isoflurane. Higher radioactive uptake was observed in the right ear of each.

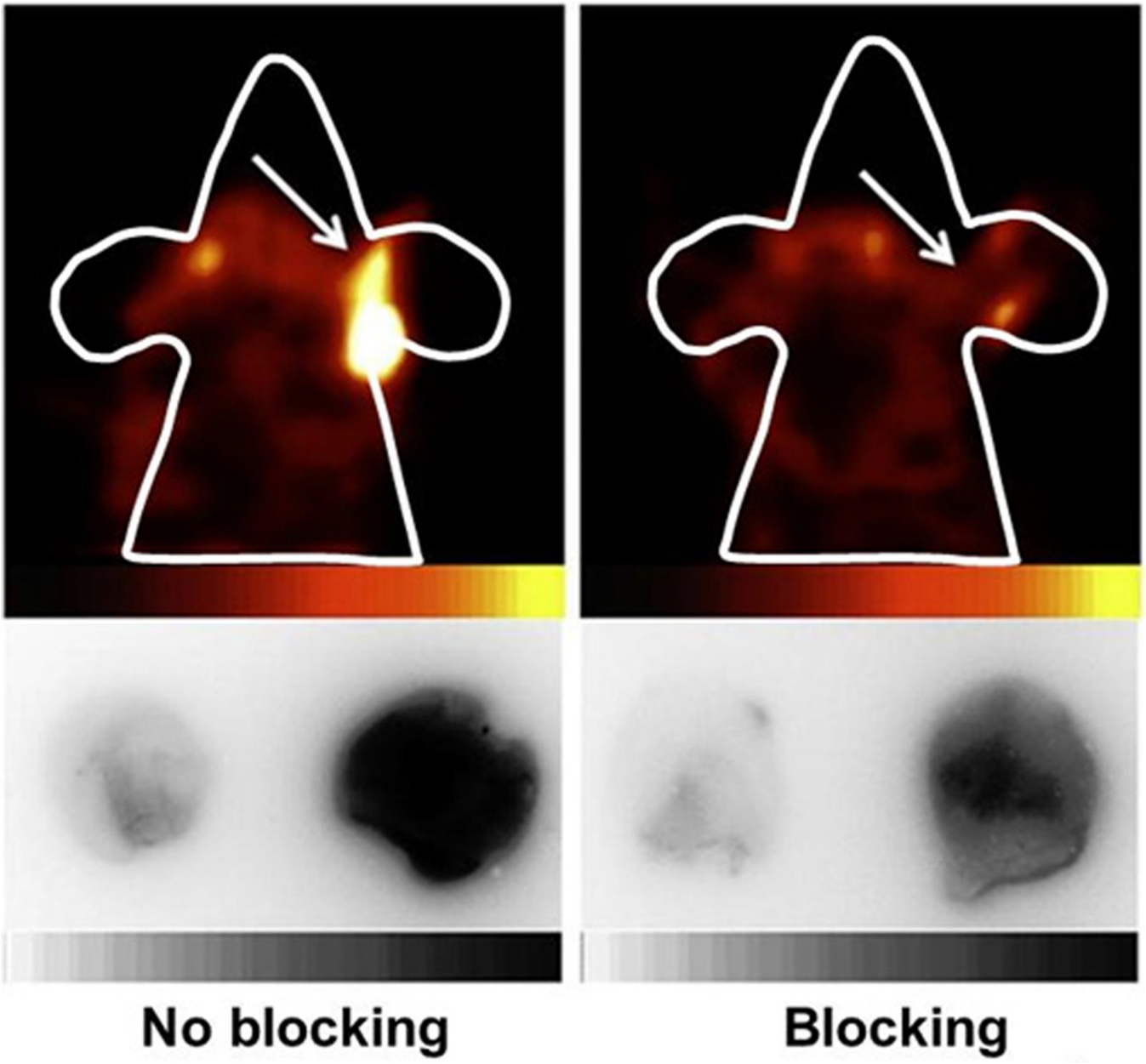

Figure 7.

Representative ^{99m}Tc-TNFR-Fc-IL-1ra SPECT (upper panel) and autoradiograph (lower panel) images in two mice with right ear TPA-induced inflammation. The mouse in the right panel received unlabeled TNFR2-Fc-IL-1ra for blockade, and the left-panel mouse received PBS as a control. The animals received 2.24 mCi radiotracer (0.2 ml) and 10-minute SPECT image acquisition. The ears showed on autoradiograph images were simultaneously exposed on the same phosphor imaging plate and the scale was set at the same quantitative value.

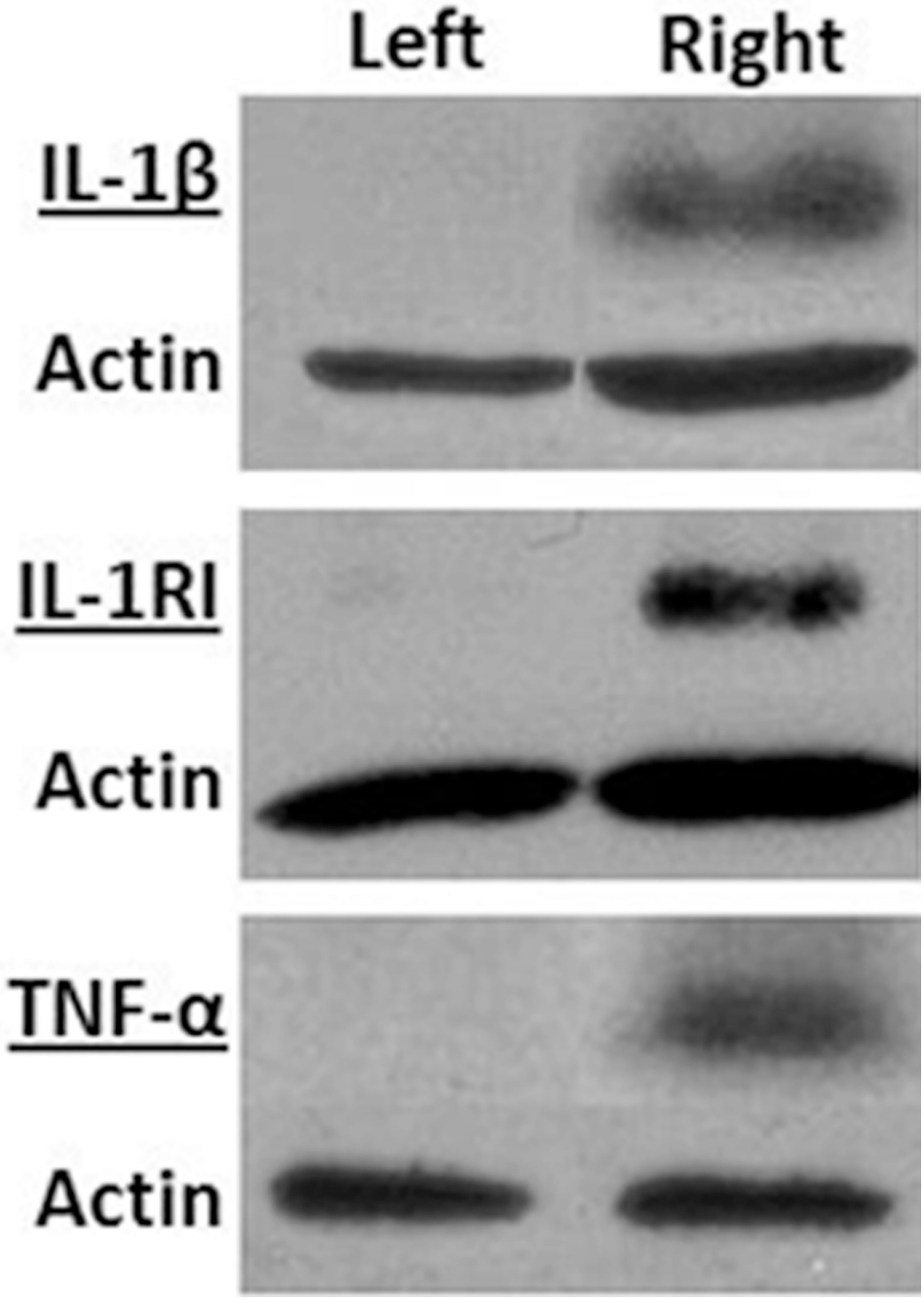

Figure 8.

Western blot analysis of interleukin-1β (IL-1β), its transmembrane receptor IL-1RI, and tumor necrosis factor-α (TNF-α) in homogenized ears that received TPA treatment (right panel) or carrier vehicle treatment (left panel). A total of 40–100 μg tissue lysates were used for western blot. IL-1β antibody (1:200 dilution), IL-1RI antibody (1:3000 dilution) and TNF-α antibody (1:10,000 dilution) were used to detect IL-1β, IL-1RI and TNFα. The figure presents data from one of two experiments with similar results.

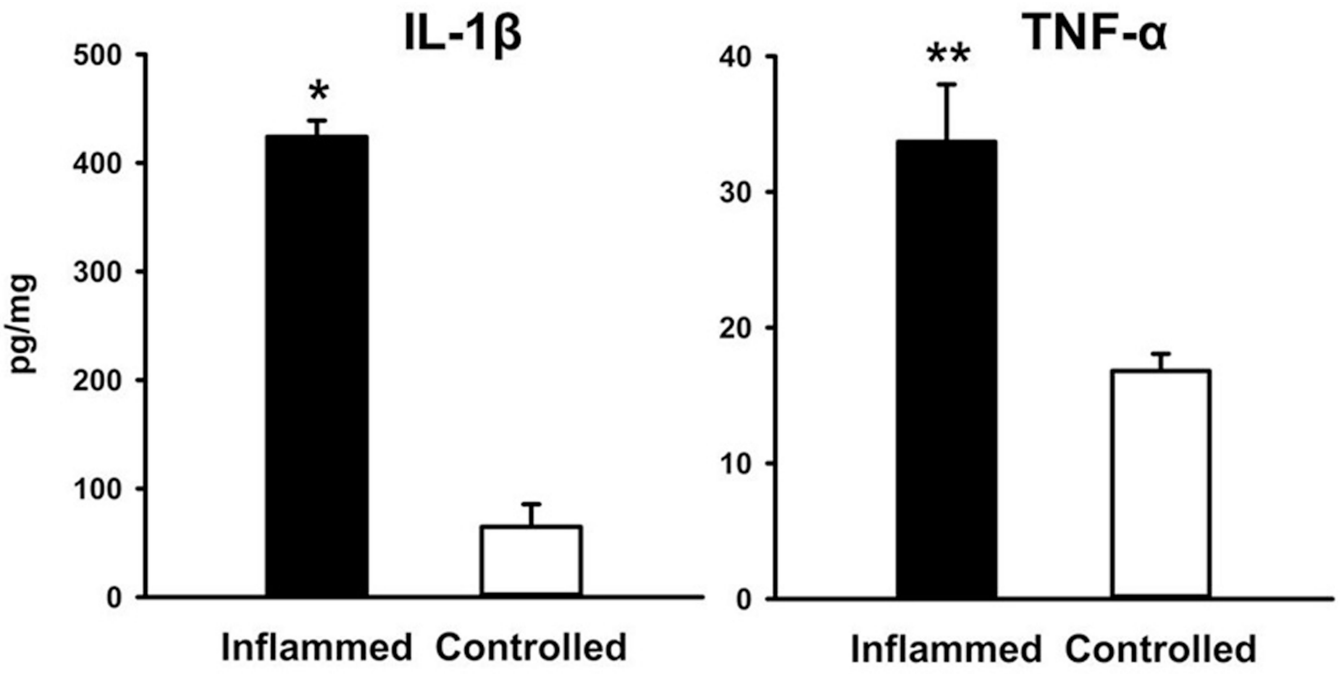

Figure 9.
ELISA detection of IL-1β and TNF-α in supernatant of homogenates from TPA-inflamed ears and control ears. Data are mean ± SEM. * and ** represent $P < 0.001$ compared with corresponding vehicle-treated ears.

Table 1

Results of ^{99m}Tc-labeled yields (%) analyzed by SG81 paper chromatography

Ratio*	**20**		**200**		**1000**		**2000**	
Solvent	**Saline**	**EAW†**	**Saline**	**EAW†**	**Saline**	**EAW†**	**Saline**	**EAW†**
IL-1ra-Fc	65.5	98.8	89.2	98.0	91.9	97.7	99.7	94.8
TNFR2-Fc	35.3	99.5	88.2	97.9	92.4	97.4	97.4	95.2
TNFR2-Fc-IL-1ra	42.7	97.5	83.1	98.6	91.4	99.0	94.4	98.2

*Molar Ratio of 2IT to protein;

†Analysis by Ethanol/Ammonia/Water = 2:1:5

Nucl Med Biol. Author manuscript; available in PMC 2013 October 01.

Table 2

Rat biodistribution data (%ID/g) of ^{99m}Tc-labeled cytokine ligands 3-hr post-injection

	TNFR2-Fc-IL-1ra	TNFR2-Fc	IL-1ra-Fc
Blood	2.07±0.07*	2.10±0.03*	1.27±0.15
Heart	0.42±0.08	0.21±0.74	0.28±0.04
Lung	0.65±0.07	0.44±0.0.003	0.45±0.03
Liver	1.43±0.03	1.29±0.17	1.40±0.04
Stomach	0.14±0.03	0.13±0.06	0.67±0.09
Spleen	0.81±0.14	0.79±0.06	0.46±0.13
Small intestine	2.39±0.66	1.50±0.48	1.24±0.36
Large intestine	0.10±0.05	0.12±0.11	0.07±0.03
Kidneys	3.79±0.01	3.82±0.08	5.18±0.66
Skin	0.07±0.01	0.13±0.09	0.09±0.02
Muscle	0.05±0.01	0.03±0.01	0.02±0.003

* represents $P < 0.05$ compared to IF.

Table 3

Thickness (μm) changes of mouse ears treated by TPA and acetone

	Right Ear		Left Ear	
	Pre-TPA	**Post-TPA**	**Pre-Acetone**	**Post-Acetone**
IL-1ra-Fc	211.4±13.5	470.0±11.3*	205.7±11.3	207.1±15.0‡
TNFR2-Fc	218.6±14.8	474.3±74.6*	202.9±15.0	208.6±9.0
TNFR2-Fc-IL-1ra	204.3±3.5	465.7±34.0*	198.6±4.8	211.4±7.0‡

* represents $P < 0.05$ compared to the remote left ear.

Table 4

Uptake of ^{99m}Tc-labeled cytokine ligands in TPA-induced mouse ear edema

	Unblocked			Blocked		
	Right Ear (R)	**Left Ear (L)**	**Ratio (R/L)**	**Right Ear (R)**	**Left Ear (L)**	**Ratio (R/L)**
IL-1ra	2.76±0.20 *	0.69±0.12	4.78±1.06	1.02±0.30 *†	0.43±0.11	2.32±0.37 ≠
TNFR2-Fc	5.86±0.40 *	2.86±0.61	2.31±0.28	4.28±0.43 *†	2.91±0.74	1.69±0.41
TNFR2-Fc-IL-1ra	7.61±0.86 *	1.99±0.31	4.13±0.53	3.61±0.35 *†	1.81±0.18	2.09±0.36 ≠

* represents $P < 0.05$ compared to the remote left ear;

† represents $P < 0.05$ compared to the right unblocked ear;

≠ represents P < 0.05 compared to unblocked Ratio.

Nucl Med Biol. Author manuscript; available in PMC 2013 October 01.